Measurement of Gamow-Teller Strength for ^{176}Yb → ^{176}Lu and the Efficiency of a Solar Neutrino Detector

M. Bhattacharya,[1,2,3,*] C. D. Goodman,[1] R. S. Raghavan,[4] M. Palarczyk,[5,†] A. García,[2] J. Rapaport,[5] I. J. van Heerden,[1,‡] and P. Zupranski[6]

[1]*Indiana University Cyclotron Facility, Bloomington, Indiana 47408*
[2]*University of Notre Dame, Notre Dame, Indiana 46556*
[3]*Nuclear Physics Laboratory, University of Washington, Seattle, Washington 98195*
[4]*Bell Laboratories, Lucent Technologies, Murray Hill, New Jersey 07974*
[5]*Ohio University, Athens, Ohio 45701*
[6]*The Andrzej Soltan Institute for Nuclear Studies, 00-689 Warsaw, Poland*
(Received 9 June 2000)

We report a 0° ^{176}Yb$(p,n)^{176}$Lu measurement at IUCF where we used 120 and 160 MeV protons and the energy dependence method to determine Gamow-Teller (GT) matrix elements relative to the model independent Fermi matrix element. The data show that there is an isolated concentration of GT strength in the low-lying 1^+ states making the proposed Low Energy Neutrino Spectroscopy detector (based on neutrino captures on ^{176}Yb) sensitive to pp and ^{7}Be neutrinos and a promising detector to resolve the solar neutrino problem.

PACS numbers: 26.65.+t, 25.40.Kv, 27.70.+q

The existing solar neutrino detectors are sensitive to different but overlapping regions of the solar neutrino spectrum. Integrated fluxes measured by these detectors [1–3] have been used to estimate the individual contributions from the pp, ^{7}Be, and ^{8}B neutrinos to the total solar neutrino flux. A model independent analysis of the current data in the framework of the standard electroweak model and the standard solar model has been performed by several authors [4–6], yielding inconsistent specific fluxes (by specific flux we mean the flux of neutrinos from a specific solar source). According to these analyses, the integrated flux observed by the Ga detectors (SAGE and GALLEX) is nearly exhausted by the low energy pp neutrino flux (which is essentially model independent) leaving no room for the ^{7}Be neutrinos. The water Cerenkov detectors (Kamiokande and Super-Kamiokande), on the other hand, observe a significant number (approximately half of their predicted value) of high energy ^{8}B neutrinos. The apparent absence of the ^{7}Be neutrinos is inconsistent with the sizable ^{8}B neutrino flux, given that ^{8}B in the sun cannot be produced without the preceding ^{7}Be$(p,\gamma)^8$B reaction. This energy dependent deficit of solar neutrinos cannot be explained by any reasonable modification of the solar model [4–6]. The most plausible solution appears to be an energy dependent (strongest at low energies) conversion of solar ν_e's to other flavors inside the Sun, viz. the MSW effect [6,7], resulting in an energy dependent distortion of the solar neutrino spectrum. Thus this idea can be fully tested only if the specific fluxes of the low energy pp and the ^{7}Be neutrinos can be measured, a task yet to be performed.

The Low Energy Neutrino Spectroscopy (LENS) detector proposed recently by Raghavan [8] will use a low-threshold, real-time, flavor-specific (using charged current neutrino capture), and spectroscopic (using a delayed coincidence technique to identify capture events from different solar sources) detection scheme based on Gamow-Teller (GT) transitions from ^{176}Yb → ^{176}Lu for measuring the specific pp and ^{7}Be neutrino flux. A measured deficit in the model independent pp neutrino flux and/or a ^{7}Be electron-neutrino flux significantly smaller than the total all-flavor flux to be measured by the BOREXINO [9] detector will provide the most direct evidence of solar neutrino flavor oscillation.

In order to estimate the neutrino capture event rates for this detector one needs an accurate knowledge of the weak interaction matrix elements for the transitions from the ground state of ^{176}Yb to the two low-lying levels in ^{176}Lu. These matrix elements can, in principle, be measured directly by using neutrinos from radioactive sources. However, a preliminary value of these matrix elements, sufficient for designing the experiment, can be deduced from intermediate energy (150 MeV/A) 0° charge exchange reactions. We report here a 0° (p,n) reaction measurement of these matrix elements.

At IUCF we measured the reaction, ^{176}Yb$(p,n)^{176}$Lu, at 0° using the IUCF neutron time-of-flight (NTOF) system in spectroscopy mode, with 120 and 160 MeV protons. We used a procedure, described in Refs. [10,11], in which the incident proton energy dependence of the ratio of the specific GT to the specific Fermi cross section is exploited to determine from the spectra the GT matrix elements relative to the model independent Fermi matrix element. It is well known that all of the Fermi strength resides in the isobaric analog state transition, which is clearly seen as a sharp peak in (p,n) spectra. The use of the energy dependence method allows us to avoid the large uncertainties (as pointed out in Ref. [10]) involved in using the globally averaged reaction cross section on a single spectrum. Figures 1(a) and 1(b) show the low energy part of

 0031-9007/00/85(21)/4446(4)$15.00

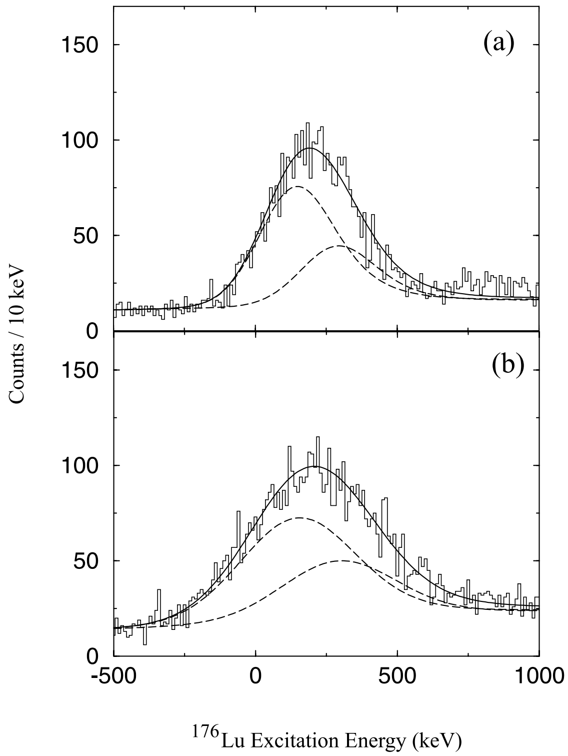

FIG. 1. Low energy part of the ^{176}Yb$(p,n)^{176}$Lu missing mass spectra, (a) using 120 MeV and (b) 160 MeV protons. Solid lines are composite fits (see text and Ref. [11] for a description of the peak shape functions) to the spectra using the peak shape parameters obtained from ^{13}N spectra. Dashed lines show the individual peaks at $E_x = 194.5$ and 339.0 keV.

the missing mass spectrum for 120 and 160 MeV protons, respectively. The data show that there is an isolated concentration of GT strength in the low-lying 1^+ states.

The level scheme of ^{176}Lu indicates that there are two 1^+ levels (with energies known from nuclear data), that are not resolved in (p,n) but resolved in a complementary $(^3\mathrm{He},t)$ experiment at Osaka [12], in this region of concentrated GT strength. The lower energy state can be populated by a significant fraction of the pp neutrinos. Hence for LENS to be able to detect the pp neutrinos it is essential that this lower energy state contain a significant portion of this GT strength. Although the two low-lying states were not physically resolved in our measurement, it is possible to separate the GT strengths to the two states by fixing the peak shape parameters to their accurately determined values from an auxiliary spectrum (described below) and by fixing the excitation energies of the two states to their well-known values. Accurate peak shape knowledge is also needed to determine precisely the number of counts in the Fermi peak used in normalizing the spectra to B(GT).

Neutron time-of-flight peak shapes are determined by the response of the detection system and the convoluted energy-time profile of the proton beam bunch. An additional effect that contributes to the peak shape is the scattering of the neutrons by the ground below the detectors. Our empirical peak shape consists of a Gaussian (accounting for the detector response, the beam energy profile, and the primary time structure of the beam bunch) convoluted with a fast exponential on either side of the Gaussian to fully take into account the time structure of the beam bunch. To take into account the contribution to the peak shape by the neutrons scattered from the ground below the detectors a long (slow) exponential was also convoluted to the low neutron energy (high excitation energy) side of the Gaussian, as these neutrons traverse a longer path than the direct neutrons. As described in more detail in Ref. [11], the counts in this tail are not from the solid angle of the detector and should ideally be removed from the analysis.

In this experiment, however, we make use only of the relative areas of the peaks corresponding to the low-lying final states and the IAS. Using only relative peak areas eliminates systematic uncertainties involved in determining absolute cross sections. The uncertainty in a peak ratio resulting from an imperfect separation of direct peak from the tail is only second order due to a possible change in the direct to scattered ratio between the unknown GT transition and the IAS peak.

As we simply ascribe a functional form to the observed peak shapes rather than modeling them from first principles, it is extremely important to test our empirical peak shape and to obtain the best values for its free parameters from an auxiliary spectrum using the same experimental setup. We chose the ^{13}C$(p,n)^{13}$N reaction because of its well-resolved level structure for this purpose. Our fit to the ^{13}N ground state using this peak shape and the Levenberg-Marquardt method [13] is shown in Fig. 2. The fit shows that our peak shape describes the data very well. We used the peak shape parameters obtained from this peak to fit the ^{176}Lu spectrum shown in Figs. 1(a) and 1(b).

As described in detail in Refs. [10] and [11], the specific Fermi and GT cross sections have a strong mass number dependence that cannot be accurately predicted by reaction dynamics theory. Hence the best way to normalize spectra to GT strengths is to normalize them to the Fermi transition. This procedure requires obtaining the number of counts in the Fermi peak which is usually not isolated or resolved from nearby and underlying GT transitions. We use the strong incident proton energy dependence of the ratio of the Fermi to GT specific cross sections to extract the number of counts in the Fermi peak. In this procedure we match spectra taken at two proton energies at a GT transition close to the Fermi peak and iteratively subtract a peak of appropriate shape from the Fermi peak in each spectrum, while minimizing a figure of merit defined to be the sum of squared differences between the two spectra. The only assumptions that go into this procedure are that the nearby peak corresponds to a pure GT transition and that the energy dependence of the ratio of specific cross sections is universal (i.e., no mass dependence).

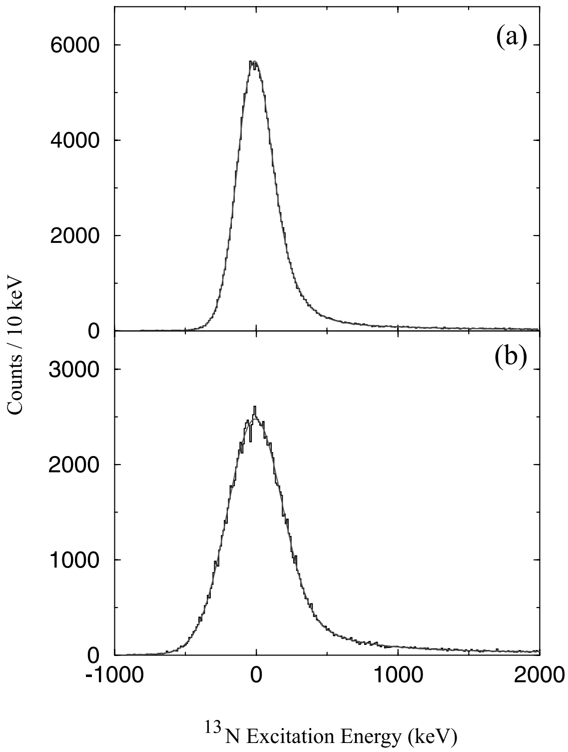

FIG. 2. Low energy part of the $^{13}C(p,n)^{13}N$ missing mass spectra, (a) using 120 MeV and (b) 160 MeV protons. Fit to the spectra using our empirical peak shape is shown. Peak shape parameters obtained from these spectra are used in the subsequent fit to the ^{176}Lu spectra.

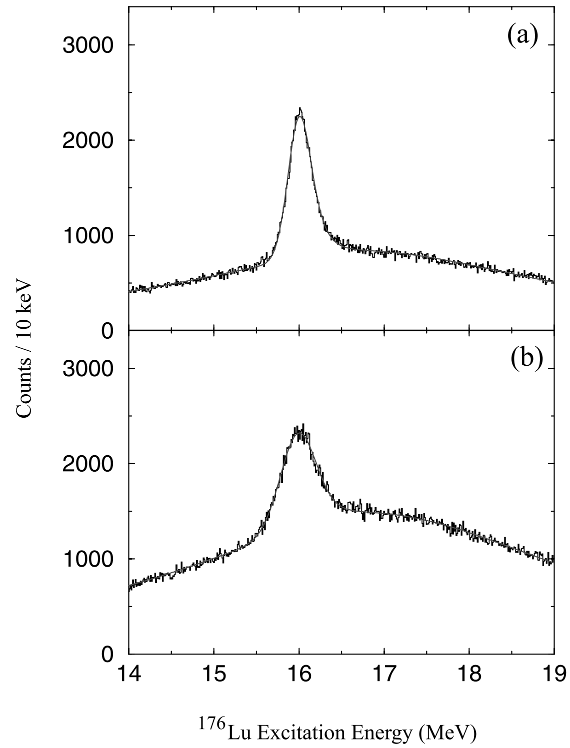

FIG. 3. High energy part of the $^{176}Yb(p,n)^{176}Lu$ spectrum (a) using 120 MeV and (b) using 160 MeV protons. Overall fit to the spectra using the empirical peak shape for the IAS peak and a Lorentzian for the GTGR is shown.

In this case (see Fig. 3) the Fermi peak rides on top of a smooth Gamow-Teller giant resonance (GTGR). Although the GTGR does not have a smooth structure in lighter nuclei, one expects it to be so in heavier nuclei as in our case. As a result, in this case one can fit the entire region containing the Fermi peak and the GTGR using our empirical peak shape for the Fermi peak and approximating the GTGR shape by a Lorentzian function. Figures 3(a) and 3(b) show our best fit ($\chi^2_{\rm min}/\nu = 1.2$) to this region for the 120 and 160 MeV spectrum, respectively, and we can see that this model describes the data very well.

We separated the GT strengths to the two states in ^{176}Lu by fixing in our fit the parameters of our empirical peak shape to their values obtained from the ^{13}N spectrum. We also fix the well-known excitation energies of the two low-lying states in ^{176}Lu. The resulting fit ($\chi^2/\nu = 1.1$) is shown in Fig. 1. The GT strengths to the two states using the areas obtained from this fit and the area for the Fermi peak obtained from Fig. 3 is given in Table I.

In the allowed approximation, the neutrino absorption cross section on ^{176}Yb is given by

$$\sigma(E_\nu) = \frac{g_V^2}{\pi \hbar^4 c^3} \sum_i p_i W_i F(Z, W_i) \left(\frac{g_A}{g_V}\right)^2 B_i(\mathrm{GT}) . \quad (1)$$

The sum runs over all ^{176}Lu daughter levels, g_V and g_A are the β-decay vector [14] and axial vector coupling constants, respectively, p_i and W_i refer to the momentum and total energy of the outgoing electron, and $F(Z,W)$ accounts for the Coulomb distortion of the outgoing electron wave function. We computed $\sigma(E_\nu)$ for the neutrino-capture reactions using the B_i values from our measurement. We calculated $F(Z,W)$ using our codes for F_0 and screening corrections and by interpolating Behrens and Jänecke's [15] L_0 value (their Table II) for finite-size corrections. Figure 4 shows the ^{176}Yb ν-absorption cross section as a function of incident neutrino energy.

Our integrated $^{176}Yb(\nu_e, e)^{176}Lu^*$ cross section over the standard (no neutrino oscillations) pp and ^{7}Be neutrino spectra is shown in Table I. LENS will also be a real-time

TABLE I. GT strengths and neutrino capture cross sections for the two low-lying states in ^{176}Lu obtained from our spectra.

		$\sigma_\nu (10^{-45})$ cm^2		
E_x(keV) [16]	B(GT)	pp	^{7}Be(0.384)	^{7}Be(0.862)
194.511 ± 0.008	0.22 ± 0.03	11.16 ± 1.53	3.35 ± 0.46	77.95 ± 10.69
338.982 ± 0.010	0.12 ± 0.02	···	···	33.11 ± 5.75

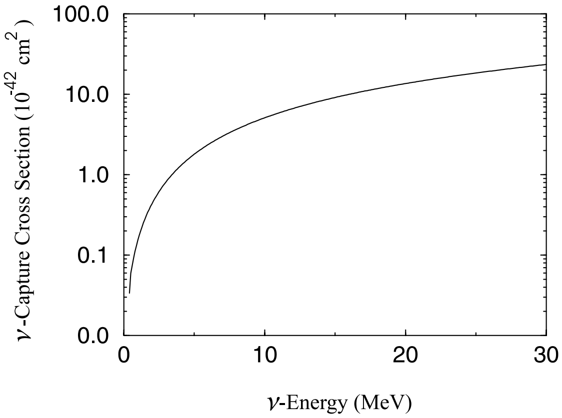

FIG. 4. Neutrino capture efficiency of LENS as a function of incident neutrino energy.

detector of supernova neutrinos and we obtain a total absorption cross section of $(5.57 \pm 0.83) \times 10^{-42}$ cm^2 for ν_e's from a Fermi-Dirac energy distribution with $T =$ 3.2 MeV (corresponding to $\langle E_{\nu_e} \rangle = 10$ MeV).

In conclusion, we measured the transition strengths of ^{176}Yb $\rightarrow$ ^{176}Lu using 0° (p, n) reactions. Our measurement indicates that the proposed LENS detector will be sensitive to the pp and ^{7}Be neutrinos. The higher energy 1^+ state in ^{176}Lu can be fed by neutrinos from all sources except the pp neutrinos, while the lower energy state can be fed by neutrinos from all solar sources including the pp neutrinos. Thus, LENS promises to be the first real-time detector capable of detecting neutrinos from the pp reaction in the Sun.

We thank Bill Lozowski for preparing the rolled foil Yb target. The IUCF and OU researchers were supported by the U.S. National Science Foundation (NSF). The Notre Dame researchers were supported by the NSF and the Warren Foundation.

*Email address: mbhattac@marie.npl.washington.edu
†Permanent address: Henryk Niewondniczański Institute of Nuclear Physics, 31-342 Kraków, Poland.
‡Permanent address: University of Western Cape, Bellville, South Africa.

[1] B. T. Cleveland *et al.,* Astrophys. J. **496**, 505 (1998).
[2] Y. Fukuda *et al.,* Phys. Lett. B **433**, 9 (1998).
[3] J. N. Abdurashitov *et al.,* Phys. Rev. Lett. **83**, 4686 (1999).
[4] Karsten M. Heeger and R. G. H. Robertson, Phys. Rev. Lett. **77**, 3720 (1996).
[5] N. Hata and P. Langacker, Phys. Rev. D **56**, 6107 (1997).
[6] J. N. Bahcall, P. I. Krastev, and A. Yu. Smirnov, Phys. Rev. D **58**, 096016-1 (1998).
[7] Peter Fisher, Boris Kayser, and Kevin S. McFarland, Annu. Rev. Nucl. Part. Sci. **49**, 481 (1999).
[8] R. S. Raghavan, Phys. Rev. Lett. **78**, 3618 (1997).
[9] *Borexino at Gran Sasso: A Real Time Detector for Low Energy Solar Neutrinos,* edited by G. Bellini and R. S. Raghavan (unpublished).
[10] T. N. Taddeucci, C. A. Goulding, T. A. Carey, R. C. Byrd, C. D. Goodman, C. Gaarde, J. Larsen, D. Horen, and E. Sugarbaker, Nucl. Phys. **A469**, 125 (1987).
[11] Charles D. Goodman, Manojeet Bhattacharya, Stewart D. Bloom, Maurice B. Aufderheide, and Pawel Zupranski (to be published).
[12] M. Fujiwara *et al.,* preceding Letter, Phys. Rev. Lett. **85**, 4442 (2000).
[13] W. H. Press, S. A. Teukolsky, W. T. Vetterling, and B. P. Flannery, *Numerical Recipes* (Cambridge University Press, Cambridge, England, 1992).
[14] G. Savard, A. Galindo-Uribarri, E. Hagberg, J. C. Hardy, V. T. Koslowsky, D. C. Radford, and I. S. Towner, Phys. Rev. Lett. **74**, 1521 (1995).
[15] H. Behrens and J. Jänecke, in *Numerical Tables for Beta-Decay and Electron Capture,* edited by H. Schopper, Landolt-Bornstein, New Series, Group 1, Vol. 4 (Springer-Verlag, Berlin, 1969).
[16] E. Browne, Nucl. Data Sheets **60**, 227 (1990).